

# Reduced-size octave-bandwidth microstrip/lumped-element rat-race coupler

Bill Slade,  
bill.slade@ieee.org

**Abstract**—By judicious choice of components, it is possible to use simple microstrip structures and a pair of lumped capacitors to realize a wideband 180 degree hybrid. The resulting structure retains the typical low-loss behavior of traditional transmission line rat-race hybrids, but by replacing the physically large 270 degree arm with a semi-lumped network, the area of the hybrid reduced by about 75% over the traditional hybrid for the given center frequency. Specifically, the long arm section of the traditional rat-race hybrid is replaced with a semi-lumped LC network in a high-pass configuration. The phase response of this high-pass LC network can be designed to closely compensate the behavior of the transmission line elements in the short arms, such that the port isolation and phasing properties are preserved over approximately an octave.

## I. INTRODUCTION

Unlike the 90 degree branch-line hybrid, the 180 degree rat-race hybrid cannot be built up from successive cascaded stages to achieve wide-band performance. Other techniques must be used, such as the  $180 - \theta$  network developed using a coplanar waveguide polarity inverter used in [1], used to achieve an impressive multi-octave response. In the interest of ease-of-fabrication, we wished to avoid the use of bond-wire or multi-layer approaches such as those used in [1], [2]. Other desirable properties that we wished to retain were low loss, reduced size over the traditional rat-race hybrid and the ability to function over approximately an octave over the range from 650MHz to 1350MHz.

The topology of the proposed wide-band coupler follows that of the standard rat-race hybrid coupler with the 270 degree loop [3] replaced with a high pass LC network like that in Figure 1 (following Gupta [4]). The method for achieving good wideband operation lies in the ability to design the compensation network such that its phase delay remains near  $180^\circ - \theta$  over the complete band (where  $\theta$  is the electrical length of the branch arms; which is defined as 90 degrees at at the center of the operating band). Furthermore, there should be as little attenuation of the signal through the network as possible so overall amplitude and phase response between the ports of the hybrid is not unduly disturbed. For this reason, we avoid the use of lumped inductors in the design.

In Figure 2, we see a typical realizable high-pass transmission response for the phase compensation network. The steep amplitude roll-off at low frequencies defines roughly the point where the hybrid will cease to function as a 3dB power splitter. The phase response follows the required  $180 - \theta$  trend that is needed for maintaining the required port to adjacent port isolation.

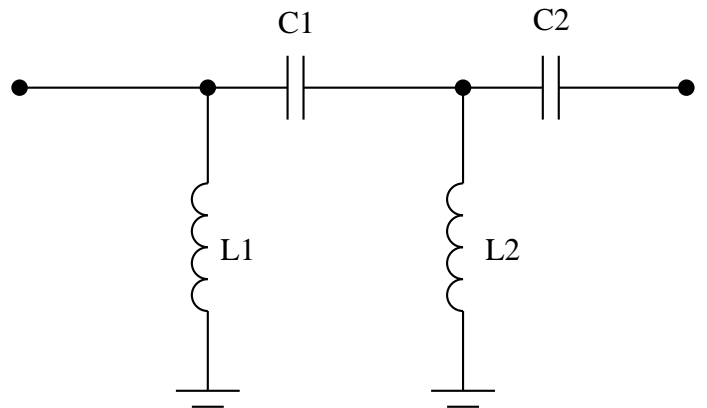


Fig. 1. Schematic of high-pass phase compensation network that is used to replace the long arm of the rat-race hybrid.

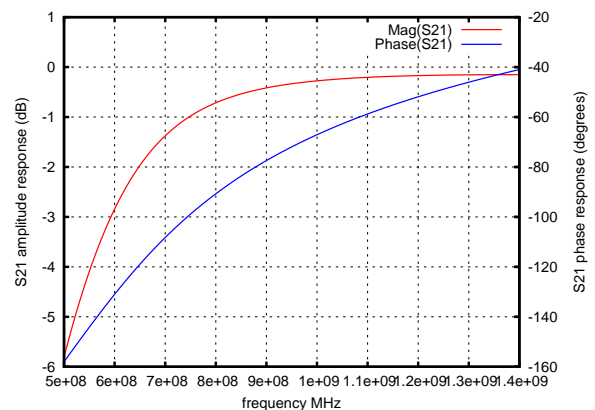


Fig. 2. Typical high-pass response for phase compensation network.

Note there are also amplitude and phase effects caused by  $S_{11}$ ,  $S_{22}$ , i.e. contributions from reflections at LC network ports. However, over most of the useful band, the reflection coefficients at the ports of the LC compensation network are relatively small compared to the transmission. The circuit model that follows and the overall optimisation that yields the component values take into account all effects during the determination of the inductor lengths and capacitor values.

The high-pass LC network is incorporated as in Figure 3. The inductors from Figure 1 are replaced with shorted shunt stubs whose lengths are determined by the center frequency of the operating band.

The capacitor values in this example are chosen for op-

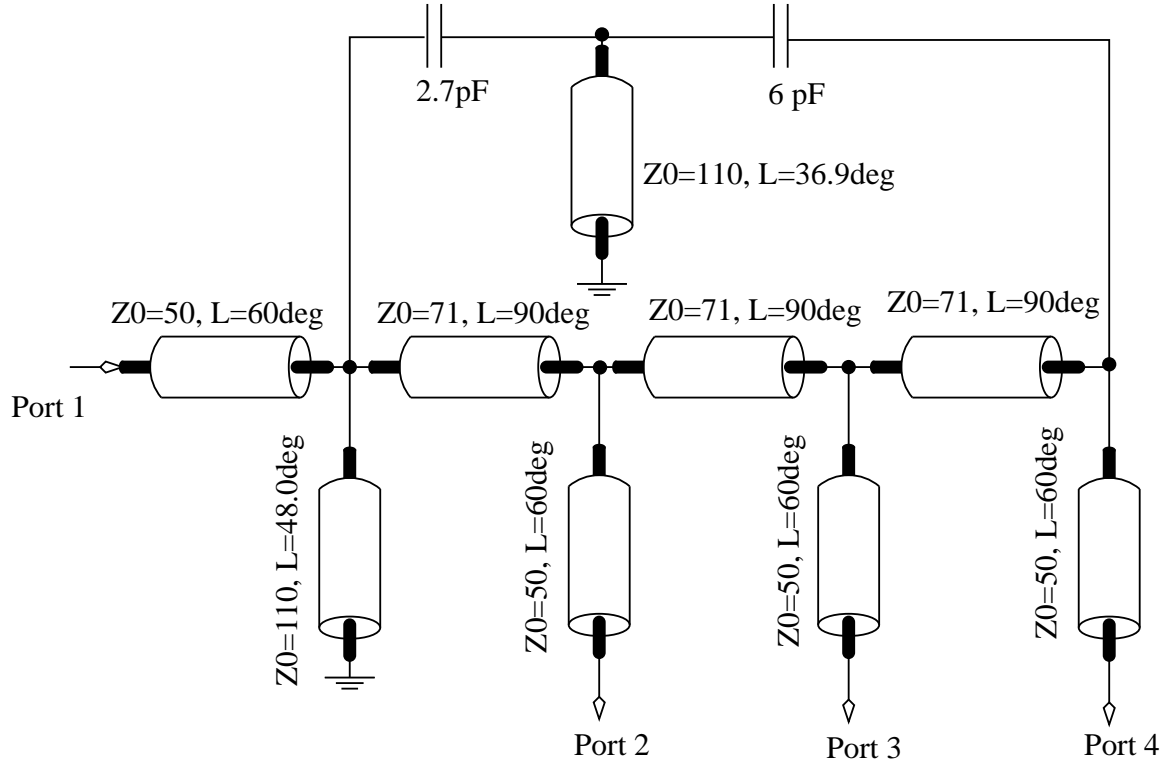


Fig. 3. Circuit diagram of rat-race coupler with lumped capacitors in long-arm "T-network." Note that the diagram shows short lengths of 50Ω line attached to the ports. This does not affect the operation of the circuit.

eration at 650-1350MHz (based on the results of a simple optimization algorithm). The ports are numbered as shown in Figure 3.

Note that the circuit as it is posed in Figure 3 does not exhibit the traditional symmetry observed in the usual rat-race hybrid. For this reason, we develop a circuit model based on two-port admittance parameters that permit a straightforward solution of Kirchoff's Current Law at each port node. The 2-port Y-parameters for transmission line segments are:

$$\mathbf{Y} = \frac{1}{jZ_R} \begin{bmatrix} \cot \theta & \csc \theta \\ \csc \theta & \cot \theta \end{bmatrix}, \quad (1)$$

where  $\theta = \beta \cdot l$  represents the electrical length of the transmission line segment ( $\beta$  is the propagation factor and  $l$ , the physical length) and  $Z_R$  is the characteristic impedance of the line.

Summing currents at each node of the circuit yields:

$$V_s = \left( 1 - j\omega C_1 R_s - \frac{R_s}{jX_L} - \frac{R_s}{jZ_R} \cot \theta \right) V_1 + \frac{R_s}{jZ_R} \csc \theta \cdot V_2 + j\omega C_1 R_s V_{LS}, \quad (2a)$$

$$0 = \frac{R_s}{jZ_R} \csc \theta \cdot V_1 + \left( 1 - 2\frac{R_0}{jZ_R} \cot \theta \right) V_2 + \frac{R_0}{jZ_R} \csc \theta \cdot V_3, \quad (2b)$$

$$0 = \frac{R_s}{jZ_R} \csc \theta \cdot V_2 + \left( 1 - 2\frac{R_0}{jZ_R} \cot \theta \right) V_3 + \frac{R_0}{jZ_R} \csc \theta \cdot V_4, \quad (2c)$$

$$0 = \frac{R_s}{jZ_R} \csc \theta \cdot V_3 + \left( 1 - \frac{R_0}{jZ_R} \cot \theta \right) V_4 + j\omega C_2 R_0 V_{LS}, \quad (2d)$$

TABLE I  
COMPONENT VALUES FOR 700-1400MHZ RAT-RACE

Variable name	Value
$\theta$	$90 \cdot f/f_{\text{center}}$ deg.
$\theta_{LS}$	$36.9 \cdot f/f_{\text{center}}$ deg.
$\theta_L$	$47.9 \cdot f/f_{\text{center}}$ deg.
$R_S$	$50 \Omega$
$R_0$	$50 \Omega$
$Z_R$	$71 \Omega$
$Z_S$	$110 \Omega$
$C_1$	$2.7\text{pF}$
$C_2$	$6.0\text{pF}$
$f_{\text{center}}$	$1 \text{ GHz}$

$$0 = -\omega C_1 X_{LS} V_1 - \omega C_2 X_{LS} V_4 + (\omega X_{LS} (C_1 + C_2) - 1) V_{LS}, \quad (2e)$$

where

$$X_L = Z_S \tan \theta_L \quad (2f)$$

and

$$X_{LS} = Z_S \tan \theta_{LS} \quad (2g)$$

The variables  $\theta_{LS}$  and  $\theta_L$  are the electrical lengths of the T-section stub and Port 1 shorted stub, respectively. Likewise,  $Z_{LS}$ ,  $Z_L$ ,  $Z_R$ ,  $R_S$ ,  $R_0$  are the T-section stub line characteristic impedance, Port 1 stub impedance, arm segment impedance, Port 1 source impedance and port 2-4 load impedances.

In developing the design, the values for the shunt stub characteristic impedances were chosen to be a conveniently fabricated high-impedance:  $100\Omega$ . The branch lines characteristic impedance is chosen to be that of the classic rat-race hybrid:  $71\Omega$ . System impedance is  $50\Omega$ . The lengths of the shunt stubs and the LC-network capacitor values are determined using a simple optimisation that is carried out based on the following optimization rules.

- 1)  $|S_{11}|, |S_{22}|, |S_{33}|, |S_{44}| < -16\text{dB}$
- 2)  $|S_{31}|, |S_{42}| < -25\text{dB}$
- 3)  $\arg(S_{21}) - \arg(S_{41}) = \pm\pi$
- 4)  $\arg(S_{23}) - \arg(S_{43}) = 0$
- 5)  $|S_{21}|, |S_{41}|, |S_{23}|, |S_{43}| = -3\text{dB}$

Capacitor values were limited to standard values and the shunt stub inductor lengths are limited to  $0 < \theta_L, \theta_{LS} < 180^\circ$ .

## II. MEASUREMENTS AND SIMULATIONS

Once suitable values are found for the unknown capacitors and shunt line lengths, a prototype is constructed on 1mm Rogers 4003 substrate (seen in Figure 4 for comparison with simulated results).

In Figure 4 we see a standard 2.4GHz rat-race hybrid on the left. It's dimensions are comparable to the proposed 650-1350MHz wideband hybrid on the right, yet the wideband hybrid will operate at a much lower frequency. The two diagonal lines are the shunt stubs, with vias to the ground plane copper. RF chip capacitors (402 package) are used to reduce the effects of physical component size.

Figures 5 and 6 show a nearly even 3dB power split between ports 2 and 4, as is predicted by the simulation. There is some

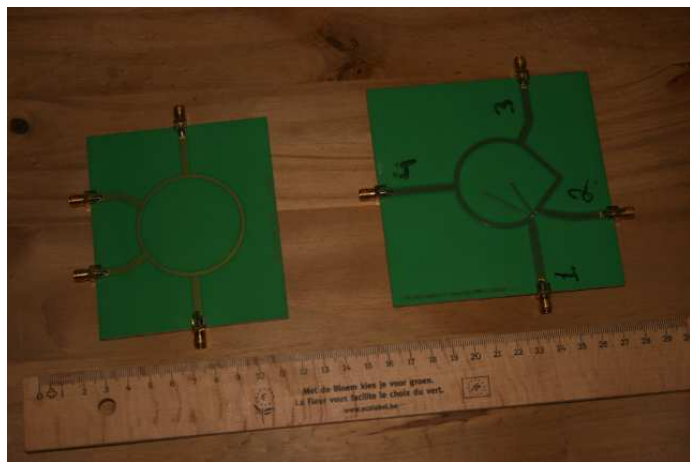


Fig. 4. Picture of 650-1350MHz wideband hybrid prototype (on the right) compared with a traditional 2400MHz rat-race hybrid (on the left). Note the shunt stub inductor placement in the wideband hybrid. Vias connect the stub ends to the ground plane underneath.

slight deviation from the simulated results at the high end of the desired band, but the amplitude error is no more than  $\pm 1\text{dB}$  from the expected simulation results. This behavior is attributed to the effects of capacitor variations as well as length and end-effects that are not included in the simple circuit model.

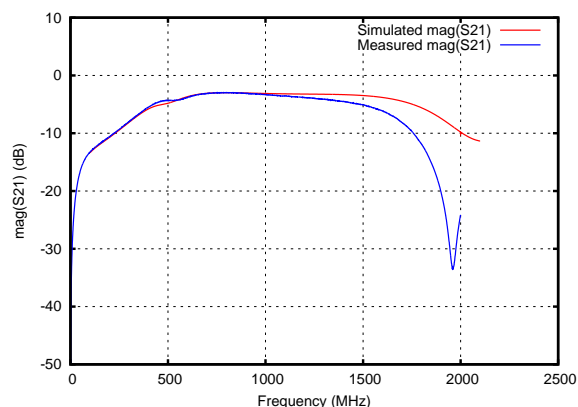


Fig. 5. Measured and simulated signal level at port 2.

The plot of  $|S_{31}|$  in Figure 7 illustrate the response of the "isolated" port 3. The simulation predicts isolation better than 25dB over the complete band. The measured results indicate isolation of better than 21dB. This was suitable for our application. However, some tuning of component values would likely improve this result.

Now that the power split and isolation properties of this structure have been established, we need to verify that the proper port phasing is present. Figure 8 shows that the phase difference between ports 2 and 4 are within a few degrees of the desired 180 degrees over the complete octave bandwidth. The maximum phase error is no more than 9 degrees. Again, tuning the capacitor values would likely improve this result.

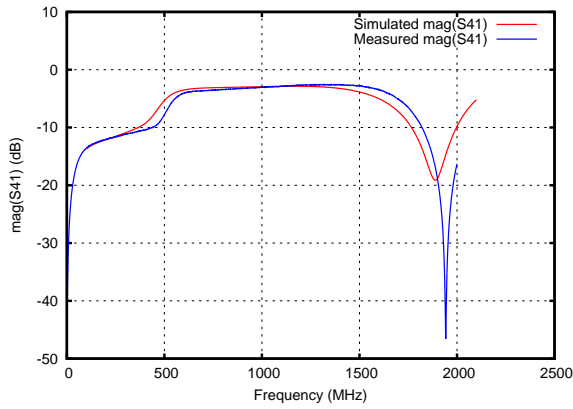


Fig. 6. Magnitude of signal output at port 4, simulated and measured.

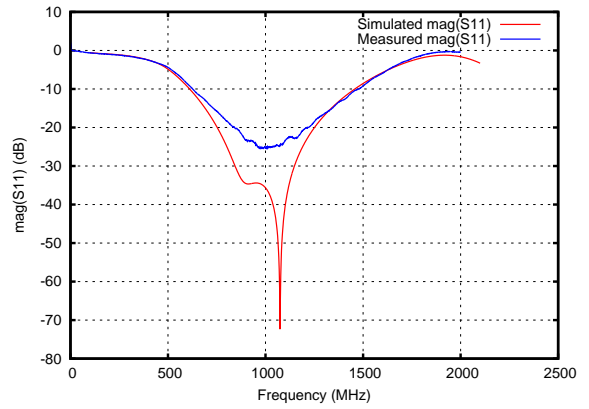


Fig. 9. The magnitude of the Port 1 reflection coefficient ( $S_{11}$ ).

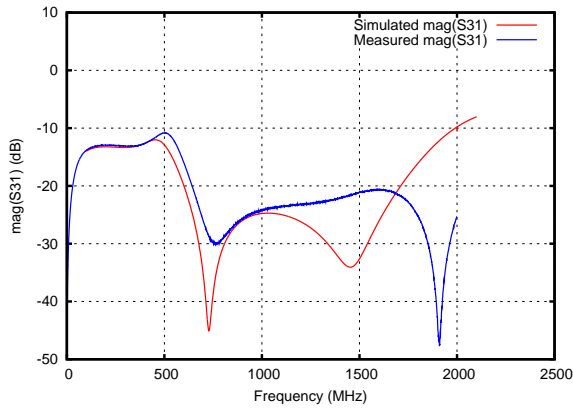


Fig. 7. Measured and simulated signal level at port 3 (isolated port).

(This is something that we avoided in order to see what performance we could achieve using unsorted commercial capacitors.)

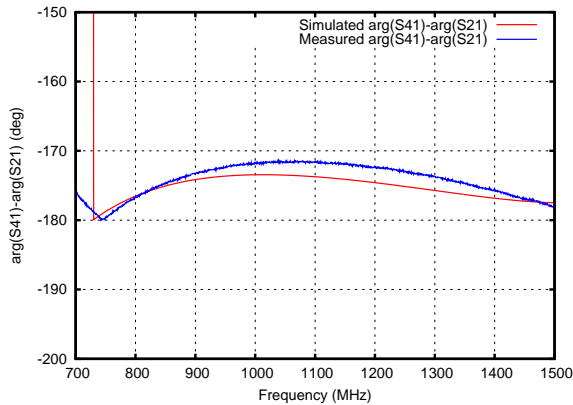


Fig. 8. The phase angle difference between port 2 and 4 outputs.

In Figure 9 we see the results for port 1 return loss. The simulated and measure results show some differences, but the reflection coefficient maintains acceptable levels ( $< -15dB$ ) over the full desired frequency range.

### III. CONCLUSION

Using conventional microstrip methods and standard value lumped capacitors, we constructed a 180 degree rat-race hybrid coupler that permits operation over somewhat more than a full octave (650-1350MHz). The power split, phase and isolation properties were reasonably well predicted using a simple circuit model. The measured performance of the hybrid is somewhat degraded toward the high end of its operating band, but still within the bounds of useful operation ( $\pm 1dB$ ,  $< 9^\circ$  phase error) for many applications. This is a result of capacitor tolerances and length effects that become apparent at short wavelengths. The circuit model used in the design did not consider these effects, but can be readily adapted if the pertinent data is available from electromagnetic simulation, for example.

Despite the simplicity of the model, it provided enough data to show the feasibility of the design and provide insight into wide-band microstrip rat-race couplers. Future work will look at extending the model somewhat to include end and length effects, loss and other candidate topologies. Of particular interest are: extending the operating bandwidth beyond an octave, extending the center frequency beyond the 1-2GHz range (where lumped capacitors become troublesome to characterise and length effects become more apparent than at "low" frequencies).

### REFERENCES

- [1] C Chang and C. Yang, "A novel broad-band Chebyshev response rat-race ring coupler," *IEEE Trans. Microwave Theory Tech.*, vol. 47, no. 4, Apr. 1999, pp. 455-462.
- [2] T. Mo, Q. Xue and C. Chan, "A broadband compact microstrip rat-race hybrid using a novel CPW inverter," *IEEE Trans. Microwave Theory Tech.*, vol. 55, no. 1, Jan. 2007, pp. 161-167.
- [3] D. M. Pozar, *Microwave Engineering*, Third edition, Wiley & Sons, 2005.
- [4] K. C. Gupta and W. J. Getsinger, "Quasi-lumped element 3- and 4-port networks for MIC and MMIC applications," *IEEE MTT-S Int. Microwave Symp. Dig.*, 1984, pp. 409-411.